RECOILLESS ABSORPTION OF GAMMA-RADIATION AND ITS APPLICATION TO PROBLEMS OF ELECTRONIC SHIELDING IN RARE EARTHS

R. L. MÖSSBAUER

Technische Hochschule, München, Germany

The method of recoilless nuclear resonance absorption of gamma-radiation provides a sensitive tool for investigations in a variety of fields, such as nuclear physics, relativity, solid state physics, chemistry and even biology. In the first part of this paper a brief introduction into the basic aspects of this method will be presented. The potentialities of the method will be illustrated in the second part by describing applications to studies of electronic shielding by closed electron shells in ionic compounds of the rare earths.

THE METHOD OF RECOILLESS ABSORPTION OF GAMMA-RADIATION

Resonance absorption of gamma-radiation in nuclei is the nuclear analogue of the well-known optical resonance phenomenon: a quantum emitted in a transition from an excited electronic or nuclear state (energy E_e) to the ground state (energy E_g) may be resonantly absorbed in an identical atom or nucleus (*Figure 1*). Recoilless nuclear resonance absorption represents a

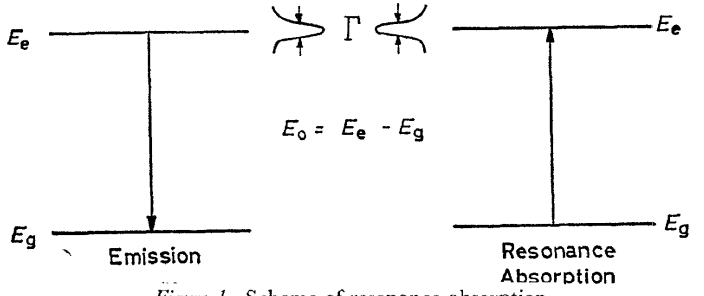

Figure 1. Scheme of resonance absorption

particular case of resonance absorption of gamma-radiation, the essential distinguishing feature of which is the fact, that the recoil momentum associated with a gamma emission or absorption process is transferred to a large system rather than to a single nucleus. This is practically achieved by employing nuclei which are strongly bound in crystal lattices[1].

The shapes and positions of gamma-lines are schematically shown in *Figure 2* for two different situations:

(*i*) In the case of free nuclei, the emission line is centred at energy $E_\gamma = E_0 - E_R$, since the conservation laws of energy and momentum

require in first order the division of the transition energy $E_0 = E_e - E_g$ into the energy E_γ of the emitted quantum and into the kinetic energy E_R of recoiling nucleus. Typically we have 10^{-2} eV $< E_R < 10^{+2}$ eV, *i.e.*

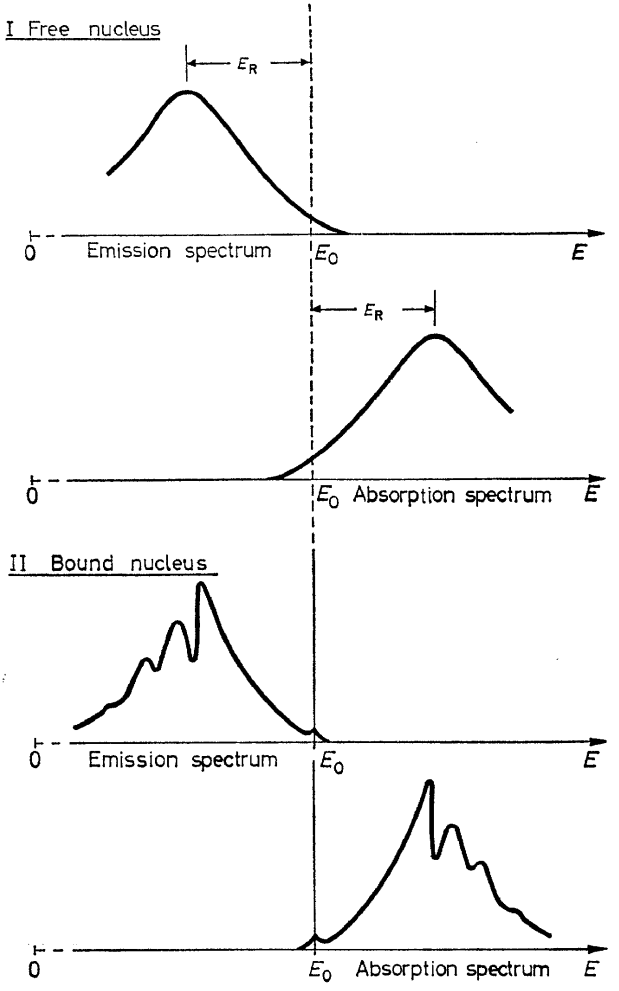

Figure 2. Schematic representation of the positions and shapes of gamma emission and absorption lines associated with nuclei which are either entirely free to recoil or bound in crystal lattices. The origin of the energy scales is suppressed

$E_R \ll E_\gamma$. Emission and absorption lines are broadened beyond their natural widths Γ by the Doppler effect, due to the thermal motions of the emitting and absorbing nuclei. The Doppler widths of gamma-lines may exceed the natural widths by factors of up to 10^{10}.

(*ii*) In the case of nuclei bound in crystals, an entirely different situation arises. The translation energy due to the transfer of momentum to the whole crystal is negligible. Energy transfers to or from the crystal are nevertheless

possible in the course of a gamma emission or absorption process due to the possibility of changes in the vibrational state of the lattice, *i.e.*, gamma transitions may be accompanied by phonon transitions. As a result, a pronounced structure appears in the gamma spectra. The different peaks in the emission spectrum shown in the lower part of *Figure 2* represent those gamma emission processes which are accompanied by, from right to left, 0,1,2 . . . . -phonon emission processes. It should be noted, that the mean energy transfer to the lattice, *i.e.*, the "mean" shifts of the emission and absorption lines towards lower and higher energies, respectively, coincide in the case of free and bound nuclei[2]. Bound nuclei, therefore, will exhibit pronounced line structures only as long as the mean "recoil" energy compares to or is smaller than typical phonon transition energies.

Of particular interest here are those transitions within the gamma emission spectra which are not accompanied at all by phonon transitions and which we therefore classify as recoilless gamma transitions. The frequency spread of these particular gamma transitions is exclusively determined by the energy uncertainty of the nuclear excited state involved, *i.e.*, these gamma transitions are represented by gamma-lines which truly exhibit the natural line width Γ.

It should be emphasized that the basic principle underlying recoilless resonance absorption of gamma-radiation, the transfer of momentum to an entire crystal while simultaneously the internal quantum state of the crystal is left unchanged, is not at all limited to this particular type of process. There exist, in fact, many other physical processes which are characterized by a momentum transfer to a bound system such, that the entire system picks up the recoil momentum without practically changing its internal quantum state. Examples are X-ray and cold neutron scattering from crystals, high energy electron scattering from complex nuclei, nucleon scattering in complex nuclei, photo-pion production in complex nuclei. In each case there exists a characteristic factor f which represents the probability for the absorption of the recoil momentum by the complex (bound) system while simultaneously no changes occur in the internal quantum state of the system. The corresponding f factors which apply to the cases of elastic X-ray and gamma resonance scattering from crystals and which are often referred to as Debye–Waller factors may for sufficiently large crystals in thermal equilibrium be written as:

$$f = e^{-\mathbf{k}^2\langle x^2\rangle} \tag{1}$$

where $\langle x^2\rangle$ is the mean square displacement in the direction of $\mathbf{k}$ of the relevant nucleus which vibrates around its equilibrium position in the lattice. The vector $\mathbf{k}$ which enters into equation (1) differs in the two cases mentioned above. For elastic scattering of X-rays $\mathbf{k} = \mathbf{k}_i - \mathbf{k}_f$, where $\mathbf{k}_i$ and $\mathbf{k}_f$ are the wave vectors of the incident and scattered X-ray waves. For gamma resonance scattering $\mathbf{k}$ represents the wave vector of the emitted or absorbed gamma-radiation. The difference in the two f factors arises from the fact, that the lifetimes of the intermediate states associated with both types of scattering processes are either short (X-ray transitions) or long (gamma resonance transitions) compared to characteristic vibrational periods of the nuclei within the crystal. In this sense, X-ray scattering and

gamma resonance scattering may be classified as "fast" or "slow" scattering processes[3].

The f factors of gamma resonance transitions depend according to equation (1) upon the ratio of $\langle x^2 \rangle$ to $\lambda\!\!\!^{-2} = (\lambda/2\pi)^2$, where λ is the wavelength of the emitted or absorbed gamma-radiation. A large f factor, *i.e.*, an unshifted line with high intensity obtains whenever, the condition holds:

$$\lambda\!\!\!^{-} \gtrsim \langle x^2 \rangle^{1/2} \tag{2}$$

Out of this condition arises a limitation of $E_\gamma \lesssim 150$ keV for the gamma energies suitable for recoilless resonance experiments.

The appearance of narrowed resonance widths, which occurs in case the inequality (2) is fulfilled, is not at all confined to the case of gamma resonance transitions. One obtains narrowed resonance widths whenever a particle emits, absorbs or scatters waves while being limited to a region in space which is comparable to or smaller than the wavelength of the radiation involved. A macroscopic example of such a situation is given by the atomic hydrogen maser[4], where a resonance narrowing was achieved by employing a cavity of 15 cm linear dimension, which approaches the wavelength $\lambda\!\!\!^{-} = 3{\cdot}4$ cm of the hyperfine transition studied. Dicke[5] in 1952 impressed condition (2) upon the one-dimensional model of an emitting atom confined to a box in order to explain the collision narrowing of optical spectral lines in a dense gas.

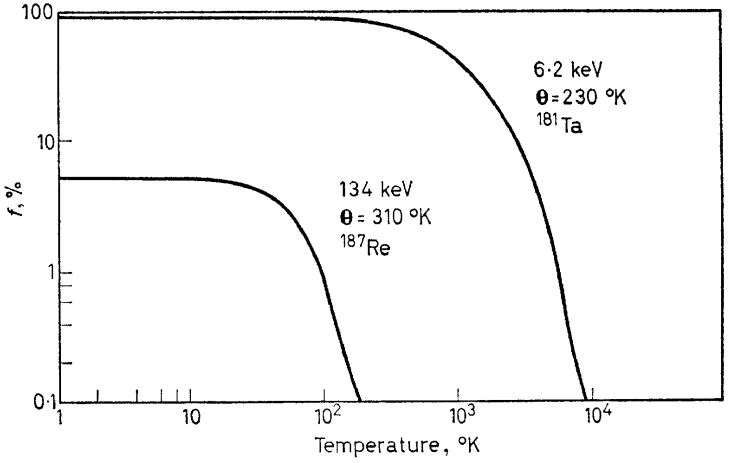

Figure 3. Temperature dependence of the f factor for the gamma transitions of lowest and highest energy which have been observed as yet in measurements of recoilless resonance absorption

The temperature dependence of the f factor derives from the temperature dependence of $\langle x^2 \rangle$. Two examples of this dependence upon temperature are shown in *Figure 3*, which is based upon the assumption of a Debye lattice vibrational spectrum for each of the monoatomic lattices. Another extreme example would be the case of a nuclear motion limited to a rather fixed range. The f factor corresponding to this situation according to equation (1) only exhibits a rather weak dependence on temperature.

The vast bulk of experimental investigations of recoilless gamma transitions have been performed via absorption measurements. *Figure 4* demonstrates the principle of such measurements. The relative motions between sources and absorbers are typically produced by means of electromechanical velocity transducers. A voltage signal of proper time dependence is fed into a drive coil, while a voltage signal proportional to the instantaneous velocity is gathered from a pick-up coil. A complete transmission *versus*

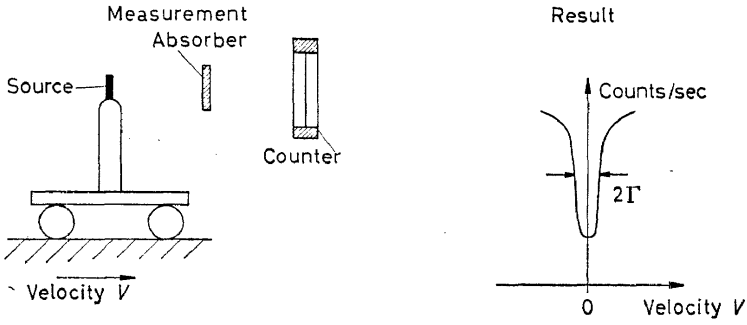

Figure 4. Principle of resonance absorption measurements. Maximum resonance absorption, *i.e.*, minimum transmitted intensity, occurs whenever emission and absorption lines are centred at the same energy. The perfect overlap of both lines may be destroyed via the Doppler effect by applying appropriate relative velocities between source and absorber. In this way one scans with an emission line of width Γ, an absorption line of width Γ, giving rise to a transmission line of width 2Γ for an infinitely thin absorber

velocity spectrum may be exhibited on the display screen of a multi-channel analyser, whose different channels have been assigned to different velocity intervals within the whole velocity range studied. Detailed descriptions of operational features of such velocity spectrometers are available in the literature[6].

APPLICATION TO PROBLEMS OF ELECTRONIC SHIELDING IN RARE EARTHS

In this section will be discussed applications of the method of recoilless resonance absorption of gamma-radiation to investigations of hyperfine interactions in isotopes of the rare earths. Specifically measurements of the contribution of closed electron shells to nuclear hyperfine interactions in salts of thulium will be discussed. Details of these measurements have been published elsewhere[7]. The investigation reported has been triggered by diverging theoretical predictions concerning the shielding which the crystal electric field at the location of the 4*f* electron shell of a rare earth ion suffers due to charge polarizations of closed electron shells. Lenander and Wong[8], Ray[9], and Watson and Freeman[10] concluded that electronic shielding plays a significant role in rare earth crystal electric field splittings. In contrast, Burns[11] concluded that electronic shielding in rare earth ions is of little importance and that the difference between the crystal field level splittings in the rare earth series and those in the iron series cannot be attributed to electronic shielding of the 4*f* electrons from the crystal field by outer closed electron shells.

Many radioactive isotopes of the rare earths emit gamma quanta in transitions to their stable ground states with energies sufficiently low to permit the observation of recoilless resonance absorption. Suitable transitions have been observed in isotopes of Sm, Eu, Gd, Tb, Dy, Er, Tm, and Yb. In many cases nuclear hyperfine interactions reveal themselves directly as a fine structure in the gamma transmission *versus* velocity curves due to the fact that the (natural) widths of the relevant gamma-lines are often smaller than the hyperfine splittings of the nuclear levels involved, in contrast to the situation prevailing in the ordinary case of Doppler-broadened gamma-lines. *Figure 5* illustrates schematically some hyperfine splittings obtainable in the case of the 8·4 keV transition in ^{169}Tm. This is an example for an

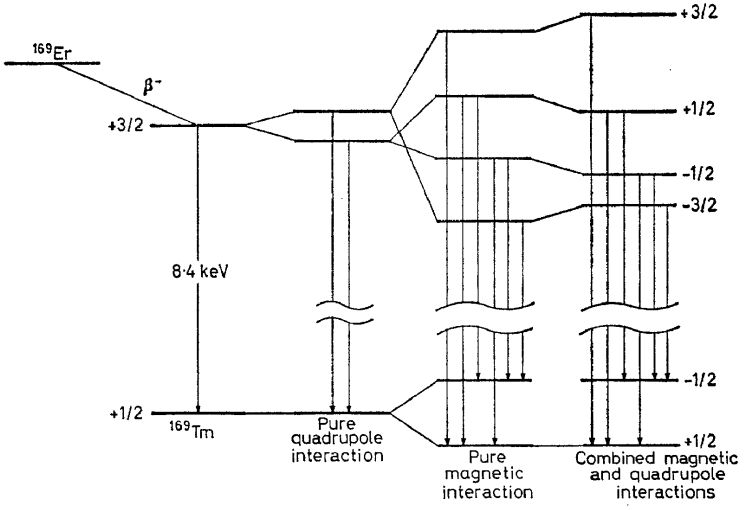

Figure 5. Decay scheme of ^{169}Er and examples of various hyperfine splittings which may be associated with the 8·4 keV gamma transition in ^{169}Tm

isotope which exhibits no quadrupole moment in the stable ground state, a fact which precludes measurements of the quadrupole interaction in thulium by resonance methods employing stable isotopes since the relative abundance of ^{169}Tm is 100 per cent. The method of recoilless resonance absorption nevertheless permits measurements of the quadrupole interaction employing ^{169}Tm, since the first excited state ($I = 3/2$) exhibits a quadrupole moment.

The nuclear hyperfine interactions in rare earth ions in crystals are strongly influenced by the interactions of the ions with the crystal electric field produced by the ions which surround the central rare earth ion in the lattice. The electronic level schemes of a free rare earth ion and of an ion bound in a crystal differ in first order only in the fact, that the directional degeneracy of the total angular momentum J is partially or completely removed in the case of the bound ion, giving rise to a number of Stark levels. The number of Stark levels is determined by the symmetry of the point group associated with the site of the rare earth ion. The overall splitting, which is determined by the strength of the crystal field interactions is

typically of order 300°K. *Figure 6* shows as an example the splitting which the electronic ground state of a free Tm^{3+} ion experiences in different crystal electric fields. The magnetic dipole moments and electric quadrupole moments of the rare earth nuclei in their ground states or excited states

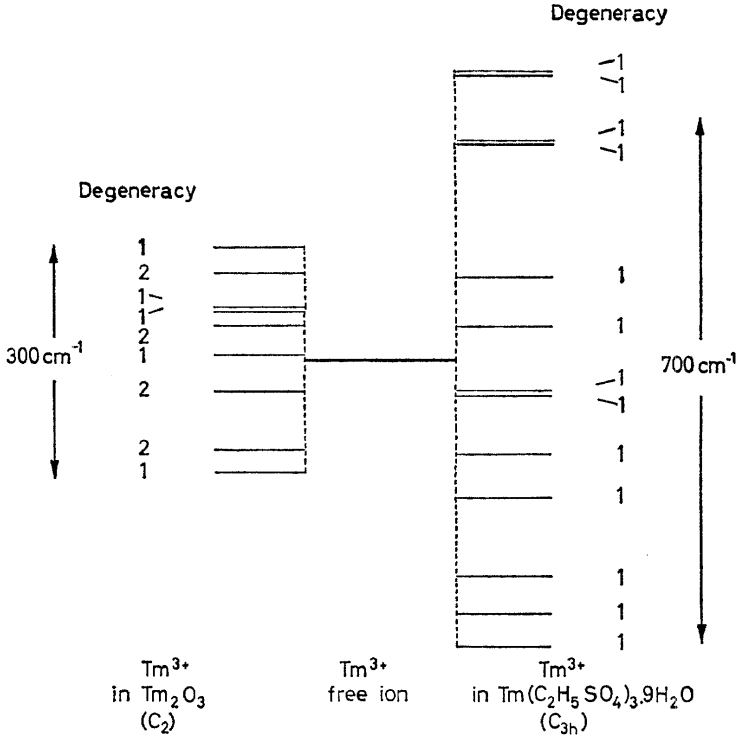

Figure 6. The crystal electric field splitting of the $^3H_6$ ground state of Tm^{3+} into different Stark levels for two crystal fields of different point group symmetries

may interact with the magnetic fields and electric field gradients prevailing at the nuclear sites. The different electronic levels yield different contributions to these internal fields. Non-degenerate electronic states, in particular, do not contribute to the internal magnetic field, due to the time reversed nature of these states. In many cases, however, experiments are conducted under conditions where spin–lattice or spin–spin relaxation rates, which cause transitions between the different Stark levels, are fast compared to nuclear Larmor precession rates. Under this condition, one does not observe instantaneous hyperfine splittings of nuclear levels. Rather, one observes quadrupole hyperfine splittings involving values of the electric field gradient which are obtained by properly averaging over the contributions from the different electronic levels, weighing each level with its appropriate Boltzmann factor. The magnetic hyperfine interactions vanish entirely, since the time reversed nature of all levels yields cancellations of

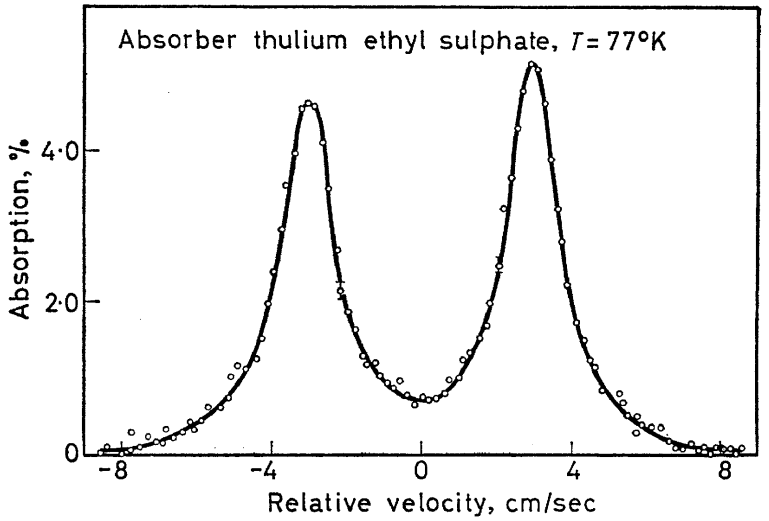

Figure 7. Quadrupole splitting of the 8·4 keV gamma absorption of thulium ethyl sulphate (5 mg/cm² of thulium) at a temperature $T = 77°K$. A source of ^{169}Er in erbium trifluoride was used at the critical temperature $T = 550°K$, where the quadrupole interaction practically vanishes, thus ensuring a "single line" source

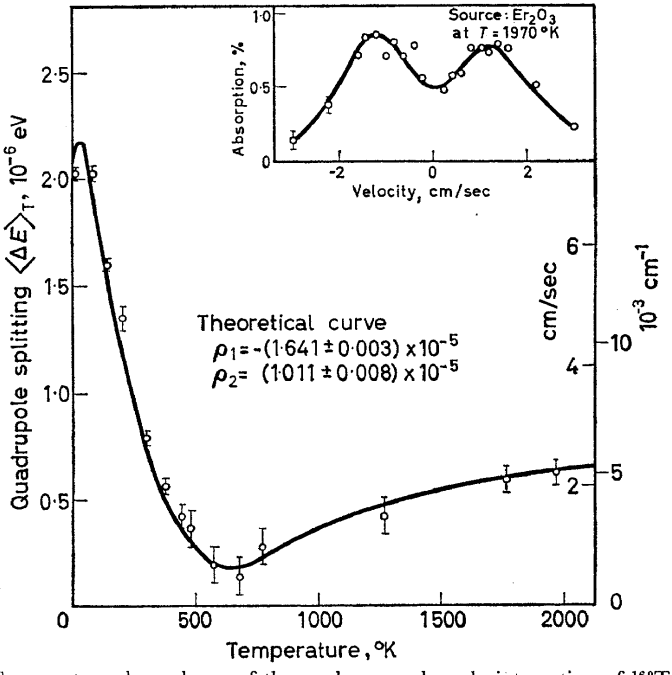

Figure 8. Temperature dependence of the nuclear quadrupole interaction of ^{169}Tm at the C_2 sites in thulium trioxide. The solid line is the best two-parameter fit (parameters ρ_1 and ρ_2) to the experimental data[7]. The insert shows a typical spectrum

contributions from $+m_J$ and $-m_J$ sub-states[12]. *Figure 7* shows an example for a pure quadrupole splitting observed under the condition of fast spin–lattice relaxation.

One might predict a reduction of the quadrupole interaction at elevated temperatures. At temperatures sufficiently high one averages over all electronic levels, thus approaching the situation of the free ion with its spherically distributed electron cloud and vanishing field gradient at its centre. The experimental points in *Figure 8* clearly disagree with this prediction. The reappearance of a strong quadrupole interaction at elevated temperatures is a drastic demonstration of the fact, that closed electron shells yield substantial contributions to the quadrupole interaction. This is the so-called Sternheimer effect[13], electronic shielding or anti-shielding of nuclear hyperfine interactions due to charge polarizations induced in closed electron shells. Analyses of measurements of the temperature dependence of the nuclear quadrupole interaction yield information on the magnitude of these Sternheimer effects, as will be outlined below.

Compiling the different contributions one may write for one component of the electric field gradient tensor:

$$eq_{ij} = (1 - \gamma_\infty)eq_{ij}^{(\mathrm{lat})} + (1 - R_Q)eq_{ij}^{(4f)} \qquad i,j = 1,2,3 \tag{3}$$

Equation (3) reflects the two essential sources of the electric field gradient which exists at the site of the rare earth nucleus:

(*i*) The gradient represented by $eq^{(\mathrm{lat})}$ which originates in the charged ions which surround a central rare earth ion in the paramagnetic crystal with a particular symmetry pattern; and

(*ii*) the gradient represented by $eq^{(4f)}$, which originates in the non-spherical distribution of the $4f$ electrons in the centre rare earth ion, caused by the non-spherical symmetry of the crystal electric field produced by the ionic environment.

The factors $-R_Q$ and $-\gamma_\infty$ in equation (3) represent, depending on their sign, reduction (shielding) or enhancement (anti-shielding) of the electric field gradients $eq^{(4f)}$ and $eq^{(\mathrm{lat})}$ respectively, due to charge polarizations of electrons in closed shells. These factors are usually referred to as Sternheimer shielding or anti-shielding factors, since Sternheimer[13] was first to emphasize the relevance of shielding phenomena caused by closed electronic shells.

The Hamiltonian $H_Q(T)$ which describes the nuclear quadrupole interaction in the principal axis system of the electric field gradient tensor, for the particular case of spin–lattice relaxation rates which are fast compared to nuclear Larmor precession rates, is given by:

$$H_Q(T) = \frac{e^2Q}{4I(2I-1)} \{[(1 - R_Q)\langle q_{zz}^{(4f)}\rangle_T + (1 - \gamma_\infty)q_{zz}^{(\mathrm{lat})}] (3\mathbf{I}_z^2 - \mathbf{I}^2) +$$

$$+ [(1 - R_Q)\langle q_{xx}^{(4f)} - q_{yy}^{(4f)}\rangle_T + (1 - \gamma_\infty) (q_{xx}^{(\mathrm{lat})} - q_{yy}^{(\mathrm{lat})})]\}\tfrac{1}{2}(\mathbf{I}_+^2 + \mathbf{I}_-) \tag{4}$$

where $\mathbf{I}$, $\mathbf{I}_z$, $\mathbf{I}_\pm$ are the usual nuclear spin operators and Q is the nuclear quadrupole moment. The quantities $\langle q_{ii}^{(4f)}\rangle_T$ represent a field gradient which obtains by averaging with their proper Boltzmann factors the field gradients associated with the different electronic Stark levels.

The following procedure was adopted in the reduction of the experimental data, which was actually performed by comparing with the Hamiltonian given by equation (4) the combined measurements of the nuclear quadrupole interaction in ^{169}Tm of Barnes *et al.*[7] and the optical measurements of Wong and Richman[14], and of Gruber, Krupke and Poindexter[15]. The analysis involved the following steps.

(*i*) The evaluation of $\langle q_{ii}^{(4f)}\rangle_T$ was performed within the magnifold of states of constant angular momentum $J = 6$, which is associated with the ground state $^3H_6$ of the Tm^{3+} ion. Admixtures of states of different J were estimated to exert but a negligible influence upon the quadrupole interaction. The field gradients $\langle eq_{ii}^{(4f)}\rangle_T$ within this approximation factorize into a radial integral $\langle r^{-3}\rangle_{4f}$ characteristic for the $4f$ electron shell of Tm^{3+} and into another factor, which carries the temperature dependence. This latter factor may be completely evaluated if the energetic position of the Stark levels (*cf. Figure 6*) is known. The latter information was taken from optical data.

(*ii*) The field gradients $eq_{ii}^{(lat)}$ were indirectly deduced by means of optical data. These data provide information on the values of $C_n^m = A_n^m\langle r^n\rangle_{4f}$, where $\langle r^n\rangle 4f$ denotes the mean value of r^n for the $4f$ electron shell and A_n^m are the parameters which appear in the usual expansion of the crystal field operator V_c which describes the potential energy at position r,θ,ϕ of a $4f$ electron:

$$V_c(r,\theta,\phi) = \sum_{n,m} \tilde{A}_n^m r^n Y_n^m(\theta,\phi) \tag{5}$$

We obtain by differentiation from equation (5) at the nuclear site ($r = 0$):

$$\begin{aligned} e^2\tilde{q}_{zz}^{(lat)} &= -4\tilde{A}_2^0 \\ e^2[\tilde{q}_{xx}^{(lat)} - \tilde{q}_{yy}^{(lat)}] &= -4\tilde{A}_2^2 \end{aligned} \tag{6}$$

It is important to note the difference between $q_{ii}^{(lat)}$ which appears in equation (4) and $\tilde{q}_{ii}^{(lat)}$ given in equation (6). This difference arises from the fact, that the definition of γ_∞ already includes the shielding contributions from all closed shells and $q_{ii}^{(lat)}$, therefore, does not include any shielding at all. The quantity $\tilde{q}_{ii}^{(lat)}$, on the other hand, already includes partial shielding, since this quantity according to equation (6) involves the crystal field parameters $\tilde{A}_2^0$ and $\tilde{A}_2^2$. These parameters are the second order terms in the crystal field expansion at the position of the $4f$ electrons, equation (5), and therefore represent a crystal field which is shielded due to the presence of closed electron shells which surround the $4f$ electrons, primarily the $5s^2p^6$ shells. We characterize this shielding effect by the factor $(1 - \sigma_2)$ and obtain

$$eq_{ii}^{(lat)}(1 - \sigma_2) = e\tilde{q}_{ii}^{(lat)} \tag{7}$$

(*iii*) The final analysis of the gamma resonance measurements of the

nuclear quadrupole interaction as a function of temperature was then performed by a two parameter least square adjustment of the measured quadrupole splitting to the theoretical splitting of the gamma-lines. This theoretical splitting was obtained by diagnolization of the Hamiltonian $H_Q(T)$, equation (4), after inserting the field gradients which have been evaluated on the basis of optical data as discussed above. The least square procedure employed the two dimensionless parameters ρ_1 and ρ_2, defined in *Table 1*, which essentially depend on the quantities $\langle r^{-3}\rangle_Q = \langle r^{-3}\rangle_{4f}$ $(1 - R_Q)$ and $(1 - \gamma_\infty)/[(1 - \sigma_2)\langle r^2\rangle_{4f}]$; the prime result of the experiment is the determination of these quantities for the two compounds studied. *Table 1* gives a compilation of experimental results and some deduced quantities.

It should be emphasized that the data presented in *Table 1* have been evaluated on the basis of certain assumptions which influence the quantities represented in various degrees. We shall now briefly appraise these assumptions.

Table 1. Semi-experimental electronic shielding factors for trivalent thulium. The following theoretical values were used in the table: $\langle J\|\alpha\|J\rangle = 0{\cdot}0102$[16]; $C_2^0 = 130{\cdot}5$ cm^{-1} for thulium ethyl sulphate and $C_2^0 = -82$ cm^{-1} for thulium trioxide; $Q = -1{\cdot}5$ barn[17]; $\langle r^{-3}\rangle_{4f} = 12{\cdot}9$[18]; $\langle r^2\rangle_{4f} = 0{\cdot}68$[19]; $\gamma_\infty = -74$[20]. Atomic units are used throughout the table

	$Tm(C_2H_5SO_4)_3{\cdot}9H_2O$	Tm_2O_3	$TmFe_2$[21]	Free Tm^{3+} ion[22]
$\rho_1 = e^2Q\langle r^{-3}\rangle_Q\langle J\|\alpha\|J\rangle/C_2^0$	$(9{\cdot}22 \pm 0{\cdot}05) \times 10^{-6}$	$-(1{\cdot}641 \pm 0{\cdot}003) \times 10^{-5}$		
$\rho_2 = Q(1 - \gamma_\infty)/\langle r^2\rangle_E$	$(1{\cdot}97 \pm 0{\cdot}05) \times 10^{-5}$	$(1{\cdot}011 \pm 0{\cdot}008) \times 10^{-5}$		
$\langle r^{-3}\rangle_Q = (1 - R_Q)\langle r^{-3}\rangle_{4f}$	10·0	11·3	9·0	
R_Q	0·22	0·12	12·5 ± 0·7	11·73
$\langle r^{-3}\rangle_M = (1 - R_M)\langle r^{-3}\rangle_{4f}$			0·03	0·09
R_M				
$(1 - \gamma_\infty)/\langle r^2\rangle_E$	370	190		
$\langle r^2\rangle_E = (1 - \sigma_2)\langle r^2\rangle_{4f}$	0·20	0·40		
σ_2	0·71	0·41		

(*i*) The evaluation of the parameters ρ_1 and ρ_2, the procedure of which has been outlined above, employs an external electrostatic potential of the form given in equation (5). This potential describes the crystal electric field outside the rare earth ion. It is assumed that this potential preserves its form also inside the ion, for instance at the position of the $4f$ electrons or at the nuclear site, the only change being the replacement of the parameters A_n^m which hold outside the ion by new parameters which depend on n and on the positions r inside the ion. In other words, the crystal electric field and the field gradients which apply inside the ion are obtained from the crystal field parameters A_n^m which apply outside by properly scaling the parameters A_n^m without otherwise changing the symmetry pattern of the potential. This procedure, which leads to the introduction of shielding factors such as $1 - \gamma_\infty$, $1 - R_Q$, $1 - \sigma_2$, is commonly referred to as *linear shielding*. The existence of non-linear shielding would invalidate the crystal field parametrization scheme employed in this analysis, as has been pointed out by Freeman and Watson[23]. Theoretical estimates of non-linear shielding are still somewhat qualitative and did not at this stage seem to facilitate corresponding corrections in our analysis. Non-linear shielding effects, therefore, have been neglected in the evaluation of the parameters ρ_1 and ρ_2.

(*ii*) The temperature dependence of the crystal field parameters $C_n^m = \tilde{A}_n^m \langle r^n \rangle_{4f}$ has been neglected throughout the analysis. The justification for this procedure is supported by measurements of Gruber and Conway[24], who determined by optical methods the energies of electronic levels of Tm^{3+} ions in thulium ethyl sulphate at $T = 77°$, 194° and 273°K. The changes with temperature in the position of the levels are typically less than 10 cm^{-1}. Furthermore, it should be pointed out that the evaluation of the experimental data relies more heavily upon the low temperature data, due to the better resolution of the quadrupole splittings which obtains at the lower temperatures. The high temperature data have in addition been separately analysed by a different method which does not rely on a knowledge of the fourth and sixth order crystal field parameters[7]. Both methods of analysis yield consistent values of ρ_1 and ρ_2 within experimental limits. It was on these grounds that it appeared justifiable to use in the analysis one set of crystal field parameters C_n^m determined optically at a single temperature.

(*iii*) The deduction of the radial integral $\langle r^{-3} \rangle_Q$ and of the quantity $(1 - \gamma_\infty)/\langle r^2 \rangle_E$ from ρ_1 and ρ_2 respectively (*Table 1*) employs a theoretical value for the nuclear quadrupole moment Q. Estimated uncertainties of 10 per cent may arise out of this.

(*iv*) The evaluation of the shielding factors R_Q and of the ratio $(1 - \gamma_\infty)/(1 - \sigma_2)$ employs theoretical values for the radial integrals $\langle r^{-3} \rangle_{4f}$ and $\langle r^2 \rangle_{4f}$ respectively. Uncertainties in these integrals may be estimated to be of the order of 10 per cent.

(*v*) The evaluation of σ_2, in addition, relies on a theoretical value for γ_∞.

(*vi*) *Table 1* also includes an evaluation of the quantities $\langle r^{-3} \rangle_M$ and R_M based upon measurements of Cohen[21]. These quantities, which characterize magnetic hyperfine interactions, do not necessarily coincide with the corresponding quantities characterizing quadrupole interactions. Measurements of $\langle r^{-3} \rangle_M$ by means of induced magnetic hyperfine interactions are in progress[25].

The results which are presented in *Table 1* and which involve certain theoretical assumptions which have been discussed above, reveal the presence of electronic shielding of the order of 20 per cent of the $4f$ electron contribution to the total field gradient at the nuclear site ("atomic" Sternheimer factor R_Q). On the other hand, the distortions induced in the closed shells by the crystal electric field lead to substantial enhancement of the direct electric field gradient produced by the surrounding ions at the nuclear site ("lattice" Sternheimer anti-shielding factor γ_∞) as well as to substantial reduction of the crystal field as seen by the $4f$ electrons (shielding factor σ_2). Values for $(1 - \gamma_\infty)/(1 - \sigma_2)$ of 250 for Tm^{3+} ions in thulium ethyl sulphate and of 130 for Tm^{3+} in thulium trioxide were obtained, corresponding to values of σ_2 of 71 and 41 respectively. Sternheimer[26] has most recently performed calculations of σ_2 for Pr^{3+} and Tm^{3+} ions, using the method of direct solution of the inhomogeneous Schrödinger equation for the perturbed wave functions. The reported value[20] of $\sigma_2 = 50$ for Tm^{3+} is in good general agreement with our results. We nevertheless wish to conclude, that while the presence of Sternheimer effects is drastically revealing itself in gamma resonance measurements of the nuclear quadrupole interaction, their

interpretation in terms of shielding factors seems at present to be somewhat limited due to insufficient knowledge about the validity of the usual crystal electric field parametrization scheme as well as due to insufficient knowledge of the accuracy of theoretical free ion radial integrals. Much more experimental and theoretical work will obviously be required.

References

[1] R. L. Mössbauer. *Z. Physik* **151**, 124 (1958); *Naturwissenschaften* **45**, 538 (1958); *Z. Naturforsch.* **14a**, 211 (1959).
[2a] H. Steinwedel and J. H. D. Jensen. *Z. Naturforsch.* **2a**, 125 (1947).
[2b] H. J. Lipkin. *Ann. Phys. (N.Y.)* **9**, 332 (1960).
[3a] G. T. Trammel. *Phys. Rev.* **126**, 1045 (1962).
[3b] R. L. Mössbauer and D. H. Sharp. *Rev. Mod. Phys.* **36**, 410 (1964).
[4] H. M. Goldberg, D. Kleppner, and N. F. Ramsey. *Phys. Rev. Letters* **5**, 361 (1960).
[5] R. H. Dicke. *Phys. Rev.* **89**, 472 (1953).
[6] For example, R. L. Cohen, P. E. McMullin, and G. K. Wertheim. *Rev. Sci. Instr.* **34**, 671 (1963); E. Kankeleit. *Rev. Sci. Instr.* **35**, 194 (1964).
[7] R. G. Barnes, E. Kankeleit, R. L. Mössbauer, and J. M. Poindexter. *Phys. Rev. Letters* **11**, 253 (1963); *Phys. Rev.* **136**, A175 (1964).
[8] C. J. Lenander and E. Y. Wong. *J. Chem. Phys.* **38**, 2750 (1963).
[9] D. K. Ray. *Proc. Phys. Soc. (London)* **82**, 47 (1963).
[10] R. E. Watson and A. J. Freeman. *Phys. Rev.* **133**, A1571 (1964).
[11] G. Burns. *Phys. Rev.* **128**, 2121 (1962).
[12] R. L. Mössbauer. *Rev. Mod. Phys.* **36**, 362 (1964).
[13a] R. M. Sternheimer. *Phys. Rev.* **80**, 102 (1950); **84**, 244 (1951); **95**, 736 (1954); **105**, 158 (1957).
[13b] R. M. Sternheimer and H. M. Foley. *Phys. Rev.* **102**, 731 (1956).
[13c] H. M. Foley, R. M. Sternheimer, and D. Tyko. *Phys. Rev.* **93**, 734 (1954).
[14] E. Y. Wong and I. Richman. *J. Chem. Phys.* **34**, 1182 (1961).
[15] J. B. Gruber, W. F. Krupke, and J. M. Poindexter. *J. Chem. Phys.* **41**, 3363 (1964).
[16] J. B. Gruber and J. G. Conway. *J. Chem. Phys.* **32**, 1531 (1960).
[17] M. C. Oleson and B. Elbek. *Nucl. Phys.* **15**, 134 (1960).
[18] M. Blume, A. J. Freeman and R. E. Watson. *Phys. Rev.* **134**, A320 (1964).
[19] B. R. Judd and I. Lindgren. *Phys. Rev.* **122**, 1802 (1961).
[20] R. M. Sternheimer. *Phys. Rev.* **132**, 706 (1963).
[21] R. L. Cohen. *Phys. Rev.* **134**, A94 (1964).
[22] E. Gerdau, W. Krull, L. Mayer, J. Braunsfurth, J. Heisenberg, R. Steiner, and E. Bodenstedt. *Z. Physik* **174**, 389 (1963).
[23] A. J. Freeman and R. E. Watson. *Phys. Rev.*, in the press.
[24] J. B. Gruber and J. G. Conway. *J. Chem. Phys.* **32**, 1178 (1960).
[25] E. Kankeleit, R. L. Mössbauer, and F. T. Snively. To be published.
[26] R. M. Sternheimer. *Bull. Am. Phys. Soc.* **10**, 597 (1965).